

STOCHASTIC ISOCURVATURE BARYON FLUCTUATIONS, BARYON DIFFUSION, AND PRIMORDIAL NUCLEOSYNTHESIS

H. Kurki-Suonio¹, K. Jedamzik², and G. J. Mathews³

¹*Research Institute for Theoretical Physics and Department of Physics, University of Helsinki, 00014 Helsinki, Finland*

²*University of California, Lawrence Livermore National Laboratory, Livermore, CA 94550*

³*University of Notre Dame, Department of Physics, Notre Dame, IN 46556*

ABSTRACT

We examine effects on primordial nucleosynthesis from a truly random spatial distribution in the baryon-to-photon ratio (η). We generate stochastic fluctuation spectra characterized by different spectral indices and root-mean-square fluctuation amplitudes. For the first time we explicitly calculate the effects of baryon diffusion on the nucleosynthesis yields of such stochastic fluctuations. We also consider the collapse instability of large-mass-scale inhomogeneities. Our results are generally applicable to any primordial mechanism producing fluctuations in η which can be characterized by a spectral index. In particular, these results apply to primordial isocurvature baryon fluctuation (PIB) models. The amplitudes of scale-invariant baryon fluctuations are found to be severely constrained by primordial nucleosynthesis. However, when the η distribution is characterized by decreasing fluctuation amplitudes with increasing length scale, surprisingly large fluctuation amplitudes on the baryon diffusion scale are allowed.

Subject headings: cosmology: theory - early universe - nuclear reactions, nucleosynthesis, abundances - large-scale structure of universe - dark matter

1. Introduction

In this paper we investigate the effects of baryon diffusion on the big bang nucleosynthesis abundance yields for models which are characterized by a randomly distributed baryon-to-entropy ratio. Such models are distinctively different from the well-studied models (Malaney & Mathews 1993) of adiabatic inhomogeneities or baryon inhomogeneities initially inspired by a first-order QCD phase transition. We discuss models both with and without the collapse of a significant fraction of the large-mass scale, high-density regions. Our study is motivated by the primordial, isocurvature, baryon (PIB) fluctuation model of structure formation (Peebles 1987ab). However, the results and constraints derived here apply to any theory which produces stochastic fluctuations in the baryon-to-entropy ratio which can be characterized by a spectral index.

Primordial, isocurvature, baryon fluctuations have been proposed (Peebles 1987ab) as a model for the formation of cosmic large-scale structure. In this model it is envisioned that at early times the universe was filled with fluctuations in the baryon-to-entropy ratio characterized by increasing fluctuation amplitudes with decreasing mass scale. PIB models with primordial power spectra of the right normalization and spectral index ($-1 \lesssim n \lesssim 0$, where $n = 0$ corresponds to white noise) may be quite successful in reproducing the statistical properties of the observed large-scale structure at the present epoch (Sugihara & Suto 1992; Cen, Ostriker, & Peebles 1993). These models have even certain advantages over other popular structure formation models (e.g. cold dark matter or mixed dark matter with $n \approx 1$) including the early formation of structure and the small peculiar velocity flows on small scales. An often invoked feature of PIB models is the collapse of Jeans-mass size ($M_J \sim 3 \times 10^5 M_\odot (\Omega_b h^2 / 0.1)$), non-linear entropy fluctuations around the epoch of recombination and the early formation of baryonic, collisionless dark matter in the form of black holes or brown dwarfs (Hogan 1993, Loeb 1993).

PIB models, however, are severely constrained by current observations of the anisotropies in the cosmic microwave background radiation. In contrast to cold dark matter or mixed dark matter models, PIB models require an early reionization (Peebles 1987a; Gorski & Silk 1989; Chiba, Sugiyama, & Suto 1993; Hu & Sugiyama 1994). Moreover, this reionization

should only be partial and occur in the right redshift range. It remains to be shown if this can be accomplished self-consistently in such models.

PIB models usually assume that the fractional contribution of baryons to the critical density is $\Omega_b \sim 0.1-0.2$ (including remnants, as well as diffuse baryons). This value is much larger than that allowed by the light element abundance constraints of a homogeneous big bang nucleosynthesis, i.e. $0.007 \lesssim \Omega_b h^2 \lesssim 0.023$, where h is the Hubble parameter in units of $100 \text{ km s}^{-1} \text{ Mpc}^{-1}$ (Smith, Kawano, & Malaney 1993; Copi, Schramm, & Turner 1995; Cardall & Fuller 1996). This fact, and the fact that the existence of entropy fluctuations in general significantly change the abundance yields during primordial nucleosynthesis, has led to at least three independent derivations of nucleosynthesis constraints on the PIB fluctuations for small mass scales (Gnedin, Ostriker, & Rees 1995; Jedamzik & Fuller 1995; Copi, Olive, & Schramm 1995). On the other hand, it had already been pointed out in earlier more schematic studies that the upper limit on Ω_b may be substantially larger than that derived from homogeneous big bang nucleosynthesis when a significant fraction of high-density regions collapse and “swallow” their high ${}^4\text{He}$ and ${}^7\text{Li}$ yields (Harrison 1968; Zeldovich 1975; Rees 1984; Sale & Mathews 1986).

Probably the most important result of all three recent investigations of big bang nucleosynthesis with stochastic entropy fluctuations and collapse is that there is no agreement between calculated primordial abundances and observationally inferred abundance limits for any Ω_b when significant fluctuation power is present on mass scales below the Jeans mass. This is because high-density fluctuations on scales smaller than the Jeans mass don’t collapse but rather expand and mix their high ${}^4\text{He}$ and ${}^7\text{Li}$ yields with the remaining diffuse baryons (Jedamzik & Fuller 1994). In other words, a simple extrapolation of the preferred stochastic PIB fluctuation spectrum to small mass scales with a spectral index ($-1 < n < 0$) seems to be ruled out by nucleosynthesis considerations.

In an attempt to circumvent this constraint, Gnedin *et al.* 1995 focussed on the possibility that entropy fluctuations are strongly phase correlated. They considered super-Jeans-mass size fluctuations described individually by a radial power law- or top hat- distribution. Retaining the stochastic nature of fluctuations Jedamzik & Fuller 1995 (hereafter; JF95) speculated on the possibility of a fluctuation cut-

off on mass scales above the Jeans mass. In both cases the authors concluded that the total Ω_b in remnants and diffuse baryons may be as large as that reflected by dynamical estimates of the density parameter, $\Omega \sim 0.1 - 0.2$ (Peebles 1986; Kaiser *et al.* 1991; Dekel *et al.* 1992; Strauss *et al.* 1992), without being in conflict with nucleosynthesis abundance constraints. This is true as long as the high-density regions collapse efficiently. JF95 also pointed out that PIB-like models can produce intrinsic, large-mass scale variations in the primordial abundances which may possibly be inferred from future observations of ($^2\text{H}/\text{H}$)-ratios in high-redshift Lyman-limit clouds (see also Jedamzik & Fuller 1996).

In any case, all previous studies did not adequately address the effects of dissipative processes during the nucleosynthesis era on the primordial nucleosynthesis yields. It is well known that baryon diffusion and hydrodynamic expansion during primordial nucleosynthesis affects the abundance yields when entropy fluctuations on mass scales, M , in the range $10^{-22}M_\odot \lesssim M \lesssim 10^{-10}M_\odot$ are present. It is, perhaps, a bold extrapolation to infer the amplitudes of entropy fluctuations on these small mass scales from the amplitudes of entropy fluctuations on mass scales relevant to structure formation ($M \gg M_J$). Nevertheless, one would expect that inflation generated spectra should extend over many orders of magnitude. And in any event, disregarding large-scale structure formation, it is instructive to know which kind of stochastic fluctuation spectra (existing with appreciable amplitudes on either only small scales or both, small and large scales) are compatible with nucleosynthesis considerations.

Gnedin *et al.* (1995) have attempted to account for dissipation during nucleosynthesis by using the small-scale, inhomogeneous nucleosynthesis yields derived by Mathews *et al.* (1990). The calculations by Mathews *et al.*, however, correspond to the abundance yields produced in a regular lattice of fluctuation sites, such as might be produced during a first order QCD transition. In contrast, the few existing baryogenesis scenarios capable of producing PIB-like fluctuations suggest a stochastic nature of fluctuations (Yokoyama & Suto 1991; Dolgov & Silk 1992). Moreover, Gnedin *et al.* used only those fluctuation parameters which optimize the upper limit on Ω_b , which is clearly an unrealistic oversimplification. JF95 attempted to qualitatively estimate the effects of dissipation during nucleosynthesis on the abundance

yields for a random entropy distribution. They suggested that the ^4He and ^7Li yields of a stochastic distribution are generally lowered by the effects of baryon diffusion but should still be higher than the corresponding yields in a homogeneous big bang nucleosynthesis scenario at the same Ω_b .

In this paper we compute primordial nucleosynthesis yields for random entropy fluctuations with different spectral indices and fluctuation amplitudes. We explicitly incorporate effects of baryon diffusion during the nucleosynthesis epoch. Our calculations serve to place constraints on the homogeneity in the baryon-to-photon ratio independent of any gravitational collapse. We also combine our results with PIB-like models of structure formation in order to derive approximate constraints on the allowed isocurvature power spectrum. In Section 2 we give the relevant physical scales entering the problem, introduce our models of stochastic baryon inhomogeneity which are based on the models of JF95, and explain our numerical techniques for the calculation of primordial abundance yields. In Section 3 we present our results and in Section 4 we draw conclusions.

2. Random Baryon Fluctuations and Primordial Nucleosynthesis

2.1. Physical Length and Mass Scales

In what follows we will give all length scales in comoving units at the present epoch. Often we will associate a length scale, λ , with a baryonic mass scale, $M_b(\lambda)$, by employing

$$M_b = \frac{\pi}{6} \bar{\rho}_b \lambda^3, \quad (1)$$

where $\bar{\rho}_b$ is the average baryon density at the present epoch. There are three relevant physical scales in our problem. First, there is the neutron diffusion length scale, $d_n(T \approx 500\text{keV})$, determined at the epoch of weak freeze-out in the early universe. This scale divides length scales, L , which have been homogenized by baryon diffusion before the onset of primordial nucleosynthesis, $L \lesssim d_n$, from length scales on which inhomogeneities in the baryon-to-photon ratio η can persist through the beginning of primordial nucleosynthesis, $L \gtrsim d_n$,

$$d_n(T \approx 500\text{keV}) \approx 4 \times 10^{-5} \text{pc}. \quad (2)$$

In deriving Eq. 2 we assume $\Omega_b h^2 \lesssim 1$ locally (see Jedamzik & Fuller 1994). Using Eq. 1 with $d_n = \lambda$,

we find the corresponding mass scale

$$M_{500\text{keV}}^d \approx 1 \times 10^{-22} M_\odot (\Omega_b h^2 / 0.0125). \quad (3)$$

The second length scale is the neutron diffusion scale at the approximate completion of freeze-out from nuclear statistical equilibrium

$$d_n(T \approx 10\text{keV}) \approx 8 \times 10^{-2} \text{pc} (\Omega_b h^2 / 0.0125)^{-\frac{1}{2}}. \quad (4)$$

This scale corresponds to a baryonic mass scale

$$M_{10\text{keV}}^d \approx 1 \times 10^{-12} M_\odot (\Omega_b h^2 / 0.0125)^{-\frac{1}{2}}. \quad (5)$$

We note here that the relevant M^d at the completion of the freeze-out process is also sensitive to the local $\Omega_b h^2$ because the termination temperature of the primordial nucleosynthesis process is itself a function of $\Omega_b h^2$. Small local $\Omega_b h^2$ imply relatively large $M^d \gg 10^{-12} M_\odot$. Regions separated by length scales, $L > d_{10\text{keV}}^n$, are not in contact through baryon diffusion during the epoch of primordial nucleosynthesis. If any one region of the universe is homogeneous on length scales $d_{10\text{keV}}^n$, but inhomogeneous on larger scales, the nucleosynthesis yields can be simply computed by an appropriate abundance average over different homogeneous big bang nucleosynthesis scenarios at different η . This is what has been done in all prior studies (Gnedin *et al.* 1995; JF95; Copi *et al.* 1995). However, when small-scale inhomogeneities are present a reliable calculation has to at least cover the length scale range from $d_{500\text{keV}}^n$ to $d_{10\text{keV}}^n$. Our calculations achieve this. Finally, there is the Jeans length

$$\lambda_J \approx 5 \times 10^{-2} \text{Mpc} \left(\frac{\Omega_b h^2}{0.1} \right)^{-\frac{1}{2}}, \quad (6)$$

yielding the Jeans mass

$$M_J^b \approx 3 \times 10^5 M_\odot (\Omega_b h^2 / 0.1)^{-\frac{1}{2}}. \quad (7)$$

The ultimate fate of overdense regions with $M \gtrsim M_J^b$ is collapse, whereas isolated, overdense regions with $M \lesssim M_J^b$ will expand and mix their nucleosynthesis yields with the remaining diffuse baryons. It should be noted that M_J^b is *not* the true Jeans mass before the epoch of recombination. It rather compares the effects of baryonic pressure with baryonic self-gravity and determines if a fluctuation will expand or contract.

It coincides with the post-recombination Jeans mass when all photon stresses can be neglected, and we loosely refer to it here as the Jeans mass.

2.2. Models of Primordial Isocurvature Baryon Fluctuations

PIB-like models may be described by the root-mean-square (rms) of the fractional variation in primordial baryon density as a function of mass scale M ,

$$\left(\frac{\delta \rho_b}{\rho_b} \right)_{\text{rms}}(M) = \left(\frac{\delta \rho_b}{\rho_b} \right)_{\text{rms}}(M_N) \left(\frac{M}{M_N} \right)^{-\frac{1}{2} - \frac{n}{6}}. \quad (8)$$

Here M_N is an arbitrary normalization mass scale, $(\delta \rho_b / \rho_b)(M_N)$ is the fluctuation rms on M_N , and n is a spectral index. For the primordial abundance calculations, however, the knowledge of the statistics of the distribution is not sufficient. Rather, we need to specify a distribution in baryon density as a function of spatial coordinate, $\rho_b(x)$. It is not a unique procedure to infer realizations of a distribution in baryon-to-entropy from Eq. 8. We follow JF95 and consider a Gaussian random variable, $A(x)$. We generate stochastic baryon-to-photon distributions, $\eta(x)$, by the relations

$$\eta(x) = \eta_N A^2(x), \quad (9)$$

or

$$\eta(x) = \eta_N A^{10}(x). \quad (10)$$

Here η_N is a normalization constant. Note that the $\eta(x)$ in Eq. 9 and Eq. 10 are chosen positive definite to avoid the introduction of antimatter domains. It has been shown in JF95 that the resultant distribution in η is highly non-Gaussian on small scales, in particular the transformations in Eq. 9 and Eq. 10 introduce phase correlations between the different Fourier modes. However, the distribution quickly approaches Gaussian character on larger scales.

We will employ a fluctuation cutoff length scale, λ_c , below which any regions are assumed to be homogeneous. As long as we choose $\lambda_c \lesssim d_{500\text{keV}}^n$, however, there will be no physical relevance to this scale since baryon diffusion prior to the nucleosynthesis epoch will provide a natural cutoff scale. Aside from any non-Gaussian character of the distribution, the statistics of the distribution is then fully described by three quantities. These are the effective spectral index n in Eq. 8, the rms fluctuation on the cutoff scale, $(\delta \rho_b / \rho_b)_{\lambda_c}$, and the magnitude of the cutoff scale, λ_c .

2.2.1. Models without Collapse

We will study three models of small-scale stochastic baryon inhomogeneity with fluctuations in η spanning a range from very small scales $\sim d_{500\text{keV}}^n$ to quite large scales well above $d_{10\text{keV}}^n$. We refer to these models as Model 1, 2, and 3. They are characterized by

$$\text{Model 1 : } n \approx -3, \left(\frac{\delta\rho_b}{\rho_b}\right)(\lambda_c) = \sqrt{2}, \quad (11)$$

$$\text{Model 2 : } n \approx -3, \left(\frac{\delta\rho_b}{\rho_b}\right)(\lambda_c) \approx 27, \quad (12)$$

$$\text{Model 3 : } n \approx -1.5, \left(\frac{\delta\rho_b}{\rho_b}\right)(\lambda_c) \approx 27. \quad (13)$$

In all three models we employ a cutoff-scale $\lambda_c = 6.8 \times 10^{-5}\text{pc}$, which is only slightly larger than $d_{500\text{keV}}^n$. Model 1 is generated by employing Eq. 9 and Models 2 and 3 are generated by employing Eq. 10. It is seen from Eq. 8 that Models 1 and 2 are chosen to have a close to scale invariant spectrum, $(\delta\rho_b/\rho_b) \approx \text{const}$. Note that these models do not incorporate any aspects of structure formation such as the collapse of high-density, super-Jeans-mass size regions. The specific realizations of the distributions characterized by Eq. 11 - Eq. 13 which are used to calculate big bang nucleosynthesis abundance yields for Models 1-3 are shown in the top panels of Figures 1-3. These panels show the spatially varying baryon-to-photon ratio divided by the average baryon-to-photon ratio as a function of spatial coordinate. In order to produce these distributions we generated 2×10^4 Fourier modes. Our simulation therefore has a dynamic length scale range of 2×10^4 .

It is evident that we examine a one-dimensional planar analogue to the full three-dimensional theory. This is a necessity in order to have sufficient length scale coverage to confidently calculate primordial abundance yields when baryon diffusion is occurring. Our results are therefore only an approximation to a three-dimensional distribution in η . Even though abundance yields in inhomogeneous nucleosynthesis have been found to be geometry dependent (Mathews et al. 1990), we expect our one-dimensional calculations to uncover the trends and magnitudes of the effects of baryon diffusion on the nucleosynthesis yields.

There is an additional uncertainty regarding the generality of our results for the abundance yields computed from the specific distributions shown in Figures 1-3. Different distributions than those shown in

Figures 1-3, albeit with the same statistical properties, may well give different results for the primordial abundance yields. We, however, expect this form of “simulation variance” (similar to the variance in simulations of the formation of large-scale structure) to be small in magnitude. Nevertheless, it should be kept in mind that particularly for the scale invariant spectra Model 1 and 2 there is a small amount of simulation variance.

2.2.2. Models with Collapse

In the second part of our study we will combine Models 1-3 for small-scale stochastic baryon inhomogeneity with large-scale PIB-like fluctuations and the collapse of overdense, super-Jeans mass size regions. We will refer to these models as Models 1C - 3C. We follow JF95 and exclude the abundance yields of regions from the abundance average, whenever the fractional variations in baryon density exceeds a critical value, $(\delta\rho/\rho) \geq \Delta_{cr}$, and when the region’s mass scale satisfies, $M > M_J^b$. As argued in JF95, for slightly non-linear, primordial fluctuations, $\Delta_{cr} \gtrsim 1$, we expect early collapse and, possibly, the formation of dark remnants.

Similarly to the spectrum of small-scale inhomogeneities, and as done in JF95, we will have to introduce a fluctuation cutoff mass scale for the large-scale PIB fluctuations. This is due to the impossibility of generating Fourier modes covering the whole mass scale range from the very small mass scales, $M \sim 10^{-22}M_\odot$, to the mass scales relevant for structure formation, $M \gg 3 \times 10^5M_\odot$. In fact, in order to calculate the abundance yields for PIB spectra with small- and large-scale power, we will only slightly modify the procedure of JF95. Whereas JF95 assumed any region with mass $M < M_J^b$ to be homogeneous, we will assume that any such region’s abundances are well approximated by the abundance yields computed from the small-scale inhomogeneous distribution shown in the top panels of Figure 1-3.

It is common practice in the field of structure formation to describe the behavior of fluctuation amplitudes on length (mass) scale by a primordial power spectrum, $P(k)$. In the absence of any significant phase correlations the rms fluctuation amplitudes in the fractional variations of primordial baryon density as a function of mass scale can be derived from the

power spectrum by

$$\left(\frac{\delta\rho_b}{\rho_b}\right)_{\text{rms}}^2(M) = \int_0^{k(M)} d\ln k k^3 P(k) . \quad (14)$$

In this expression we derive the relationship for $k(M)$ from Eq. 1 with $\lambda = (2\pi/k)$, corresponding to sharp k -space filtering. The approximate primordial fluctuation power per unit logarithmic wave vector interval (e.g. $k^{3/2}P^{1/2}(k)$) which characterizes our models of inhomogeneous nucleosynthesis and the collapse of overdense regions are shown in Figure 4. Note that the figure shows the assumed truly primordial and unprocessed power spectra. In particular, any micro-physical processing and, for example, different gravitational growth factors for different Fourier modes, usually accounted for by a transfer function, are not included.

The behavior of these models on the nucleosynthesis scale is shown on the left hand (large k) side of Figure 4, whereas the behavior of the models on the large scales relevant for collapse is shown on the right hand (small k) side of Figure 4. The cutoff for each model is shown on the right. In this figure it can be seen that the extended mass scale range in our problem forced us to resort to rather contrived power spectra. In particular, all three models do not have any fluctuation power on length scales roughly in the range $1\text{pc} \lesssim \lambda \lesssim 1\text{Mpc}$. These power spectra, however, do approximate a scenario with a white noise ($n = 0$) large-scale tail, turning over to a scale-invariant spectrum ($n = -3$) slightly above the Jeans-mass scale, and either staying scale-invariant through the scales relevant for diffusion during nucleosynthesis (Model 1C, 2C), or having a second turnover on these scales approaching spectral index $n = -1.5$ (Model 3C).

Specifically, Models 1C-3C are characterized by the following parameters:

$$\begin{aligned} \text{Model 1C : } \quad n_s \approx -3; \quad \left(\frac{\delta\rho_b}{\rho_b}\right)(\lambda_c^s) &= \sqrt{2} \times \sqrt{2}; \\ \lambda_c^s &= 6.8 \times 10^{-5}\text{pc} , \quad (15) \\ n_l \approx 0; \quad \left(\frac{\delta\rho_b}{\rho_b}\right)(\lambda_c^l) &= \sqrt{2}; \\ \lambda_c^l &= 6.8 \times 10^{-1}h^{-1}\text{Mpc}; \quad \Delta_{cr} = 1.5 , \end{aligned}$$

$$\begin{aligned} \text{Model 2C : } \quad n_s \approx -3; \quad \left(\frac{\delta\rho_b}{\rho_b}\right)(\lambda_c^s) &= \sqrt{2} \times 27; \\ \lambda_c^s &= 6.8 \times 10^{-5}\text{pc} , \quad (16) \end{aligned}$$

$$\begin{aligned} n_l \approx 0; \quad \left(\frac{\delta\rho_b}{\rho_b}\right)(\lambda_c^l) &= 27; \\ \lambda_c^l &= 9.5 \times 10^{-2}h^{-1}\text{Mpc}; \quad \Delta_{cr} = 2 , \end{aligned}$$

$$\begin{aligned} \text{Model 3C : } \quad n_s \approx -1.5; \quad \left(\frac{\delta\rho_b}{\rho_b}\right)(\lambda_c^s) &= \sqrt{2} \times 27; \\ \lambda_c^s &= 6.8 \times 10^{-5}\text{pc} , \quad (17) \\ n_l \approx 0; \quad \left(\frac{\delta\rho_b}{\rho_b}\right)(\lambda_c^l) &= 27; \\ \lambda_c^l &= 9.5 \times 10^{-2}h^{-1}\text{Mpc}; \quad \Delta_{cr} = 2 . \end{aligned}$$

Here the upper lines for each model give the parameters for the small-scale fluctuations, whereas the lower lines give the parameters for the large-scale fluctuations. Note that the small-scale distribution of Model 1C (2C, 3C) is identical to the small-scale distribution of Model 1 (2, 3). The factors of $\sqrt{2}$ in the $(\delta\rho/\rho)(\lambda_c^s)$ have only been written to illustrate that the large-scale fluctuation rms has to be added to the small-scale fluctuation rms in quadrature. The cutoff scales λ_c^l and fluctuation amplitudes $(\delta\rho_b/\rho_b)(\lambda_c^l)$ have been chosen such that the PIB fluctuation parameters are roughly normalized to yield an rms in the fractional variation of baryon density on the scale $8h^{-1}\text{Mpc}$ of unity at the present epoch (JF95). Here we assumed full reionization. It is evident that the chosen cutoff scales for the large-scale PIB-fluctuations satisfy $\lambda_c^l > \lambda_J$.

2.3. Numerical Techniques for the Calculation of Primordial Abundance Yields

The small-scale inhomogeneous nucleosynthesis calculations made use of the nucleosynthesis code developed by Kurki-Suonio *et al.* (1989, 1990a, 1990b, 1992). The nuclear reaction rates were updated according to Kawano *et al.* (1993). Regarding weak reaction rates, we used the Wagoner (1973) polynomial for the weak reaction rates, with $\tau_n = 887.0\text{s}$. We included all recently determined corrections to this rate as relevant (Dicus *et al.* 1982; Kernan & Krauss 1994; Seckel 1993; Kernan 1993). We also corrected for effects of finite spatial resolution and time step effects. The net correction factor to Y_p from all of these effects was only -0.0012. (Note that the correction +.0017 found by Kernan (1993) by using a shorter time-step does not apply to our code since the code used here is independent from the one used by Kernan.) We use all the relevant diffusion coefficients for protons and neutrons as given by Jedamzik &

Fuller (1994). However, we do not incorporate the effects of late-time hydrodynamic expansion and neutrino cooling of inhomogeneities into our calculations (Jedamzik, Fuller, & Mathews 1994) which renders our calculated (${}^7\text{Li}/\text{H}$) ratios somewhat higher than when hydrodynamic expansion is included.

A key challenge in the present work was the necessity to utilize a very large spatial grid (40 000 zones). It was thus essential to optimize the speed of computations. We therefore included only the 8 most important light isotopes in our reaction network. The reactions leading to isotopes heavier than $A=7$ were included as sinks in the reaction flow. Since there is little flow from heavier isotopes back to lighter, this is an excellent approximation for the present application. The most time consuming part of the nucleosynthesis calculation is the inversion of an 8×8 reaction matrix which must be performed at each zone at each time-step. Since this inversion does not easily vectorize, we found it best to run on a fast scalar machine.

3. Results

In this section we present the results of our inhomogeneous primordial nucleosynthesis calculations. Figures 1-3 show the employed random distributions in $\eta(x)/\langle\eta\rangle$ for the small-scale baryon inhomogeneities of Models 1-3 (and Models 1C-3C) in the top panels. Nucleosynthesis yields for the various isotopes and models are given along the side panels of Figures 1-3. The three panels on the left-hand-side of the figures give the ${}^4\text{He}$ mass fraction, Y_p , (${}^2\text{H}/{}^1\text{H}$) -number ratio, and (${}^7\text{Li}/\text{H}$) -number ratio as a function of average baryon-to-photon ratio η for the models without collapse. The three panels on the right-hand-side of the figures give the abundance yields for the same light elements as a function of baryon-to-photon ratio for the models with collapse. For reference the fractional contribution of baryons to the critical density, Ω_b , can be obtained from the baryon-to-photon ratio η by $\Omega_b = 0.0112(\eta/3 \times 10^{-10})h^{-2}$.

3.1. Models without collapse

For the panels on the left-hand-side the three lines correspond to: Solid lines—the results of a homogeneous big bang nucleosynthesis (hereafter; BBN) calculation at the same average η ; Dotted lines—the results of an inhomogeneous BBN calculation of the distribution shown in the top panel of the figure but *without* taking into account of the effects of baryon

diffusion; and Dashed lines—the results of our inhomogeneous BBN calculations which include the effects of baryon diffusion.

In the left-hand-side panels of Figure 1 we show nucleosynthesis yields for Model 1. It is seen that the abundance yields of the inhomogeneous BBN Model 1 are not very different from the yields of a homogeneous BBN scenario at the same average η (with the possible exception of ${}^7\text{Li}$). This is mainly because the fluctuation amplitudes in Model 1 are relatively small. The trends in Model 1 can be best understood when compared to the results of Model 2 which are shown in the left-hand-panels of Figure 2. Note that both Model 1 and 2 have an approximately scale-invariant spectrum ($n \approx -3$) but that Model 2 has much larger fluctuation amplitudes than Model 1. It is evident, particularly from the results of Model 2, that for close to scale-invariant spectra baryon diffusion does *not* significantly change the calculated abundance yields. This can be inferred by comparing the calculated abundance yields of the inhomogeneous distribution where baryon diffusion is accounted for (dashed line) to those where baryon diffusion is neglected (dotted line). This trend is also observed in Model 1 (Figure 1). That baryon diffusion is comparatively unimportant can be understood by inspection of the baryon distributions in Figure 1 and 2. The bulk of the baryon number in both models is included in fairly extended high-density regions with only relatively small variations in η around the approximate average baryon-to-photon ratio of these extended regions. It is known that the effects of baryon diffusion are maximized when significant fluctuations exist on scales comparable to the neutron diffusion scale during the epoch of primordial nucleosynthesis (Applegate, Hogan & Scherrer 1987). The effects of baryon diffusion on Models 1 and 2 are small since the typical length scale of extended high-density regions is much larger than the neutron diffusion length scale.

For most η values the ${}^7\text{Li}$ yields are substantially higher for the inhomogeneous distribution than the corresponding ${}^7\text{Li}$ yields in a homogeneous BBN scenario. This is a generic feature of inhomogeneous primordial nucleosynthesis (Alcock et al. 1987). Because of this, inhomogeneous BBN scenarios are only compatible with observations if there is moderate to significant depletion of ${}^7\text{Li}$ in low-metallicity Pop II halo stars. In fact, there may be evidence for ${}^7\text{Li}$ depletion in Pop II halo stars (Pinsonneault et al. 1992). However, the situation remains unresolved

(Schramm & Mathews 1996).

If one allows for the possibility of ${}^7\text{Li}$ depletion, and assumes that the primordial (${}^2\text{H}/{}^1\text{H}$) -ratio is as large as may have been inferred from some (but not all) observations of deuterium in Lyman-limit clouds at high redshift (Songaila et al. 1994; Rugers & Hogan 1996; but see also Tytler, Fan, & Burles 1996; Burles & Tytler 1996), Model 1 is marginally consistent with observations for some range in η . In contrast, Model 2 has no range in η consistent with the observationally inferred light-element abundances. We conclude that the fluctuation amplitudes of stochastic, approximately scale-invariant baryon inhomogeneities, are severely constrained by the possible overproduction of ${}^4\text{He}$ and/or ${}^7\text{Li}$ during the epoch of big bang nucleosynthesis even when the effects of baryon diffusion are included.

In Model 3 we assumed a fluctuation spectrum with spectral index $n \approx -1.5$ and with significant fluctuation amplitudes. In contrast to Models 1 and 2 this model is characterized by decreasing fluctuation amplitudes with increasing length scale as evident from the η distribution shown in the top panel of Figure 3. In a similar fashion to Figures 1 and 2 the left-hand-side panels of Figure 3 show the abundance yields of Model 3.

The results of Model 3 are, perhaps, somewhat startling. It is evident from comparison of the dotted and dashed lines in Figure 4 that for the parameters employed in Model 3 baryon diffusion *significantly* changes the abundance yields. In particular, the ${}^4\text{He}$ mass fraction in Model 3 is very close to that of a homogeneous BBN scenario and much smaller than the calculated ${}^4\text{He}$ mass fraction for the inhomogeneous distribution when baryon diffusion is neglected. For most of the range in η ${}^7\text{Li}$ yields are substantially smaller and deuterium yields are larger than those in inhomogeneous BBN scenarios without diffusion.

The effects of baryon diffusion are important since significant fluctuation amplitudes exist on the scale of the neutron diffusion length during the epoch of primordial nucleosynthesis. Fluctuations on larger spatial scales, which are much less affected by neutron diffusion and which may grossly overproduce ${}^4\text{He}$ and ${}^7\text{Li}$, are substantially smaller than those on the neutron diffusion length due to the large spectral index of the distribution. In other words, the average η in extended regions is close to the average baryon-to-photon ratio for the whole distribution.

Assuming high ${}^2\text{H}$ and significant ${}^7\text{Li}$ depletion in Pop II halo stars there is some range for η in Model 3 which can agree with all the observationally inferred primordial abundance yields. This is quite surprising since it implies that random variations in the baryon-to-entropy with rms amplitude as large as $(\delta\rho_b/\rho_b) \sim 30$ on $d_{500\text{keV}}^p$ are not ruled out by the observations of ${}^2\text{H}$, ${}^4\text{He}$, and ${}^7\text{Li}$ in low-metallicity environments. Nevertheless, if in future it is shown convincingly that either the primordial $({}^2\text{H}/{}^1\text{H})_p \approx 3 \times 10^{-5}$ is low or the primordial $({}^7\text{Li}/\text{H})_p \approx 2 \times 10^{-10}$ is low, then significant baryon-to-entropy fluctuations during the epoch of primordial nucleosynthesis are probably ruled out. This applies for both, inhomogeneities in a nearly regular lattice (such as might be generated by a first-order QCD phase transition), or stochastic inhomogeneities of arbitrary statistical properties as may be generated during inflation.

3.2. Models with collapse

We now turn our attention to the results of Models 1C, 2C, and 3C which incorporate the collapse of overdense, large-scale regions. The abundance yields from such overdense, super-Jeans-mass size regions will be excluded from the abundance average since these regions either may form black holes, brown dwarfs, and/or stellar remnants, or might undergo sufficient early stellar processing and chemical evolution which would render the regions unsuitable for the determination of primordial abundances (JF95). The results for the primordial abundances of Model 1C, 2C, and 3C are presented in the right-hand-side columns of Figure 1, 2, and 3, respectively. Each panel in these figures shows the results for: Dotted lines – a model which does not have any sub-Jeans-mass size fluctuation power as in JF95; Dashed lines – a model which includes fluctuations on scales below the Jeans length and explicitly treats diffusion as specified in Section 2; and for comparison, Solid lines – the results of a standard homogeneous BBN calculation.

As already discussed in detail in JF95, models which have a fluctuation cutoff above the Jeans mass, and which have high efficiencies for collapse of overdense regions, generally yield substantially lower ${}^4\text{He}$ mass fractions Y_p , higher $({}^2\text{H}/{}^1\text{H})$ -number ratios, and comparable to higher $({}^7\text{Li}/\text{H})$ -number ratios than a homogeneous BBN scenario. The modifications to these results by the introduction of small-scale power on scales below the Jeans scale studied here are evident from the dashed lines. In general,

small-scale fluctuations enhance ${}^4\text{He}$ and ${}^7\text{Li}$ yields over those yields from PIB models without small-scale power. This is easily understood since regions fluctuating in η mostly yield larger Y_p and (${}^7\text{Li}/\text{H}$) ratios (even when baryon diffusion is included) than regions which are homogeneous in η (as apparent from the left-hand-side panels of Figures 1-3).

If PIB models with collapse and small-scale fluctuations even exceed the ${}^4\text{He}$ and ${}^7\text{Li}$ yields of a standard homogeneous BBN scenario largely depends on rms fluctuation amplitude. Whereas Model 1C is marginally compatible with observationally inferred primordial abundances Models 2C and 3C, which have large rms amplitudes in η , either overproduce ${}^7\text{Li}$ and/or ${}^4\text{He}$ for large η or overproduce deuterium for small η . It is evident that none of the models which include small-scale fluctuations can agree with observations for large average baryon-to-photon ratios ($\eta \gtrsim 3 \times 10^{-10}$) mainly due to an overproduction of ${}^7\text{Li}$. This is not the case for PIB models which are homogeneous on scales below the Jeans scale (JF95). This implies that the introduction of small-scale fluctuations into stochastic PIB models considerably narrows, or even excludes, the ranges of η which may have agreed with observationally inferred primordial abundances for models without small-scale fluctuations.

4. Conclusions

We have investigated the primordial nucleosynthesis process for models which include random variations in the baryon-to-photon ratio. Our study explicitly accounts for the effects of baryon diffusion. Analyzing three different stochastic distributions in η , which have different fluctuation amplitudes and spectral indices, we have found that the statistical properties of stochastic baryon-to-photon inhomogeneities are severely constrained by the possible overproduction of either ${}^7\text{Li}$ and/or ${}^4\text{He}$ for large average η or deuterium for small average η . In particular, we have found that the rms amplitudes of scale-invariant η distributions, characterized by almost equal fluctuation amplitudes on all scales, are constrained to be not larger than a few.

In contrast, the constraints on the rms amplitudes of distributions characterized by decreasing fluctuation amplitudes with increasing mass scale are much weaker. In such models rms amplitudes as large as ~ 30 on the neutron diffusion scale at weak freeze-out

are currently not ruled out by observationally inferred primordial abundance limits. Nevertheless, these constraints may be considerably tightened if it is ever convincingly shown in the future that either depletion of primordial ${}^7\text{Li}$ in low-metallicity halo stars is negligible or that the primordial deuterium-to-hydrogen ratio is low (${}^2\text{H}/{}^1\text{H}$) $\sim 3 \times 10^{-5}$.

In the second part of our study we have considered stochastic baryon inhomogeneity extending from the very small baryon diffusion scale during the epoch of primordial nucleosynthesis to very large scales above the post-recombination Jeans length, and the early collapse of overdense super-Jeans-mass size regions. In agreement with JF95 we have found that significant fluctuation amplitudes on scales below the Jeans scale considerably narrow (or exclude) the parameter space of such PIB-like models which may agree with observationally inferred primordial abundance limits otherwise. We conclude that PIB fluctuations may only be consistent with observationally inferred primordial abundance limits for large Ω_b if either fluctuations are highly phase correlated (Gnedin *et. al.* 1995) or if there exists a fluctuation cutoff on scales above the Jeans scale (JF95).

This work was performed in part under the auspices of the US Department of Energy by the Lawrence Livermore National Laboratory under contract number W-7405-ENG-48. Work at University of Notre Dame was supported in part by DOE Nuclear Theory grant DE-FG02-95ER40934. Computation was done in part at the Center for Scientific Computing (Finland).

REFERENCES

- Alcock, C. R. Fuller, G. M. & Mathews, G. J. 1987, ApJ, 320, 439
- Applegate, J. H., Hogan, C. J., and Scherrer, R. J. 1987, Phys. Rev. D, 35, 1151
- Burles, S. & Tytler, D. 1996, astro-ph/9603070
- Cardall, C.Y. & Fuller, G.M. 1996, ApJ, in press
- Cen R., Ostriker J.P., & Peebles P.J.E. 1993, ApJ, 415, 423
- Chiba, T., Sugiyama, N., & Suto, Y. 1994, preprint UTAP-93-165
- Copi, C.J., Schramm, D.N., & Turner M.S. 1995, Science

- Copi, C.J., Olive, K.A., & Schramm, D.N. 1995, 451, 51
- Dekel, A., Bertschinger, E., Yahil, A., Strauss, M.A., Davis, M., & Huchra, J.P. 1992 preprint
- Dicus, D.A., Kolb, E.W., Gleeson, A.M., Sudarshan, E.C.G., Teplitz, V.L., & Turner, M.S. 1982, Phys. Rev. D, 26, 2694
- Dolgov, A. & Silk, J. 1993, Phys.Rev. D, 47, 4244
- Gnedin, N.Y., Ostriker, J.P., & Rees, M.J. 1995, 438, 40
- Gorski, K.M. & Silk, J. 1989, ApJL, 346, L1
- Harrison, E.R. 1968, A.J., 73, 533
- Hogan, C.J. 1993, ApJL, 415, L63
- Hu, W. & Sugiyama, N. 1994, preprint CfPA-TH-94-16
- Jedamzik, K. & Fuller, G.M. 1994, ApJ, 423, 33
- Jedamzik, K. & Fuller, G.M. 1995, ApJ, 452, 33.
- Jedamzik, K. & Fuller, G.M. 1996, submitted
- Jedamzik, K., Fuller, G.M., & Mathews, G.J. 1994, ApJ, 423, 50
- Kaiser, N., Efstathiou, G., Ellis, R., Frenk, C., Lawrence, A., Rowan-Robinson, M., & Saunders, W. 1991, MNRAS, 252, 1
- Kawano L.H., Smith, M.S., & Malaney, R.A. 1993, ApJS, 85, 219
- Kernan, P.J. 1993, Ph.D. thesis, Ohio State University
- Kernan, P.J. & Krauss, L.M. 1994, Phys. Rev. Lett., 72, 3309
- Kurki-Suonio, H. & Matzner, R.A. 1989, Phys. Rev., D39, 1046
- Kurki-Suonio, H., Matzner, R.A., Olive, K.A., & Schramm, D.N. 1990a, ApJL, 353, L406
- Kurki-Suonio, H. & Matzner, R.A. 1990b, Phys. Rev., D42, 1047
- Kurki-Suonio, H., Aufderheide, M.B., Graziani, F., Mathews, G.J., Banerjee, B., Chitre, S.M., & Schramm, D.N. 1992, Phys. Lett., B289, 211
- Loeb, A. 1993, ApJ, 403, 542
- Malaney, R. A. & Mathews, G. J. 1993, Phys. Rep., 229, 145
- Mathews, G.J., Meyer, B.S., Alcock, C.R., & Fuller, G.M. 1990, ApJ, 358, 36
- Peebles, P.J.E. 1986, Nature, 322, 27
- Peebles, P.J.E. 1987a, ApJL, 315, L73
- Peebles, P.J.E. 1987b, Nature, 327, 210
- Pinsonneault, M., Deliyannis, C. P., and Demarque, P. 1992, ApJS, 78, 179
- Rees, M.J. 1984, in *Formation and Evolution of Galaxies and Large Structures in the Universe*, editor D.Reidel Publishing Comp.,pg 271
- Rugers, M. & Hogan, C. J. 1996, astro-ph/9603084
- Sale, K.E. & Mathews, G.J. 1986, ApJL, 309, L1
- Schramm, D. N. & Mathews, G.J. 1996, in *Proc. 1994 Snomass Summer Study on Nuclear and Particle Astrophysics in the Next Millennium*, E. W. Kolb and R. D. Peccei, eds., (World Scientific; Singapore) 479
- Seckel, D. 1993, Bartol preprint BA-93-16, hep-ph/9305311
- Smith, M.S., Kawano, L.H., & Malaney, R.A. 1993, ApJS, 85, 219
- Songailia, A., Cowie, L. L. Hogan, C. J., & Rugers, M. 1994, Nature, 368, 599
- Strauss, M.A., Yahil, A., Davis, M., Huchra, J.P., & Fisher, K. 1992, ApJ, 397, 395
- Suginohara, T. & Suto, Y., 1992, ApJ, 387, 431
- Tytler, D., Fan, X., & Burles, S. 1996, astro-ph/9603069
- Wagoner, R.V. 1973, ApJ, 179, 343
- Yokoyama, J. & Suto, Y. 1991, ApJ, 379, 427
- Zeldovich, Ya. B. 1975, Soviet Astr. Lett., 1, 5

Figure Captions

This 2-column preprint was prepared with the AAS L^AT_EX macros v4.0.

Fig. 1.— Baryon-to-photon distribution (top panel) and nucleosynthesis yields for Model 1 (left) and Model 1C (right side panels). A value of unity on the ordinate of the top panel corresponds to $2 \times 10^4 \lambda_c$ for Model 1 (or $2 \times 10^4 \lambda_c^s$ for Model 1C), where λ_c (λ_c^s) is specified in the text. The side panels give the calculated ${}^4\text{He}$ mass fraction Y_p , (${}^2\text{H}/{}^1\text{H}$) -number ratio, and (${}^7\text{Li}/\text{H}$) -number ratio as a function of the average η . The left-hand side panels give results for the model without collapse (Model 1). The dashed lines are for the inhomogeneous distribution when baryon diffusion is included. The dotted lines are for the inhomogeneous distribution when baryon diffusion is neglected. For comparison, the solid lines are abundance yields for a homogeneous BBN calculation. The panels on the right-hand-side show the abundance yields for models with collapse of high density regions (Model 1C). The dashed lines are for an inhomogeneous distribution with collapse when small-scale fluctuation as shown in the top panel are present. The dotted lines are for an inhomogeneous distribution with collapse when there are no small-scale fluctuations. The solid lines are for a homogeneous BBN calculation. Note that the large-scale fluctuation part of Model 1C is not shown in this figure.

Fig. 2.— Same as Figure 1, but for Model 2 and Model 2C.

Fig. 3.— Same as Figure 1, but for Model 3 and Model 3C.

Fig. 4.— Illustration of the primordial fluctuation power per unit logarithmic wave vector interval $P^{\frac{1}{2}}(k)k^{\frac{3}{2}}$ as a function of wave vector k for the models employed in the nucleosynthesis calculations. The steeply sloping lines on the far left are a simple extrapolation of a PIB model with $n = 0$. This extrapolation is disrupted as indicated for the three models. At the nucleosynthesis scale, three possible fluctuation spectra are considered as described in the text.

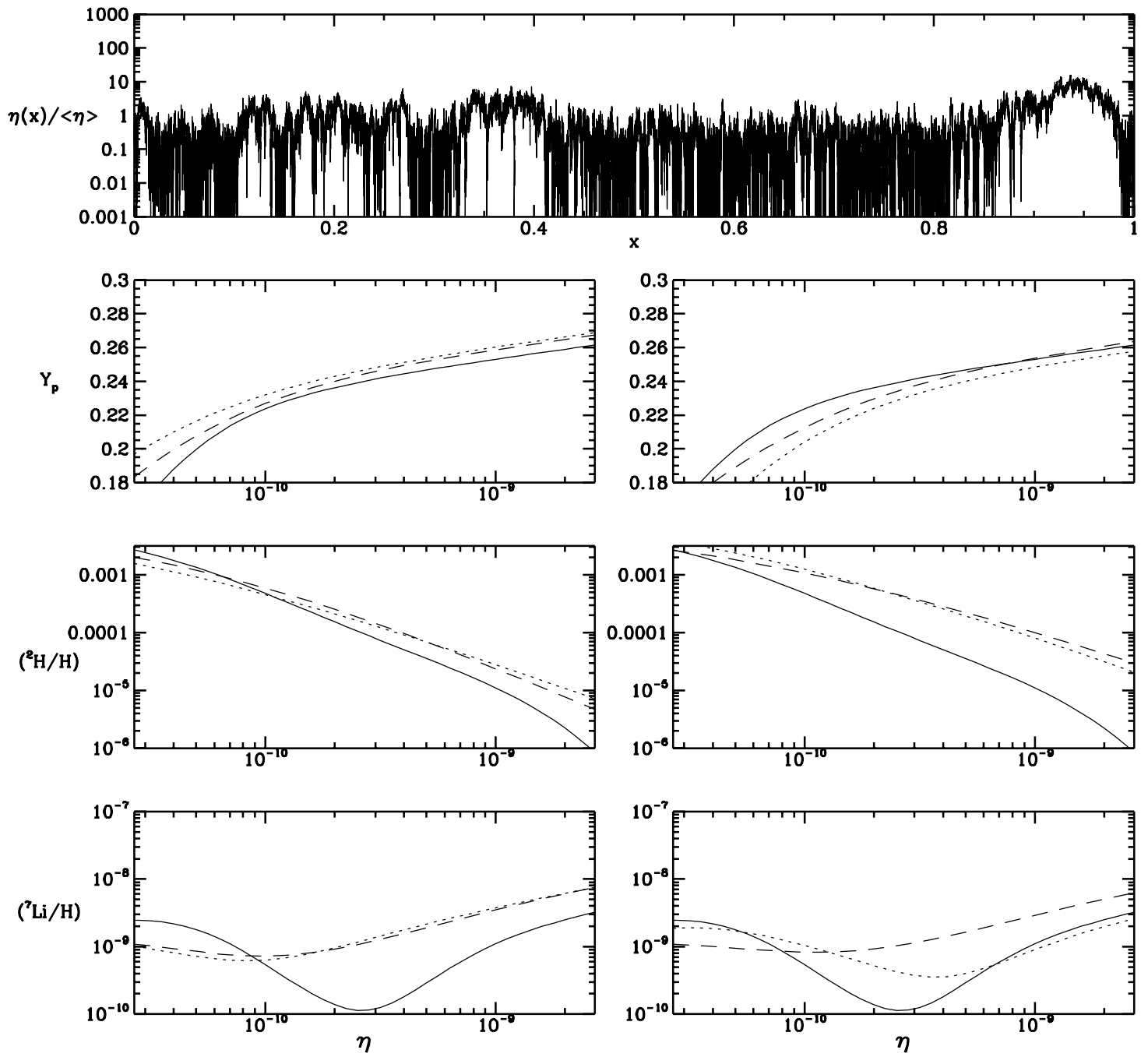


Figure 1

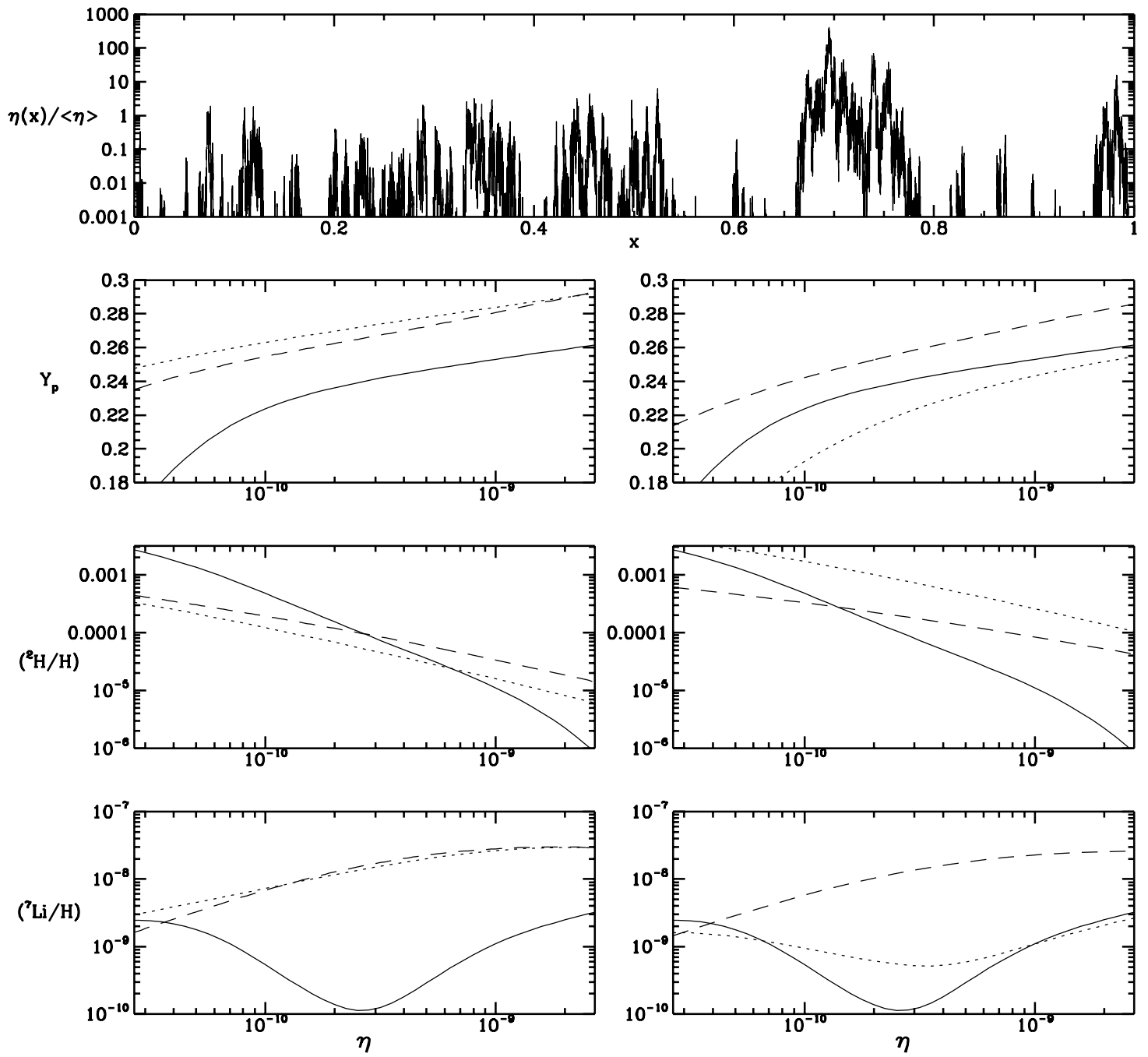


Figure 2

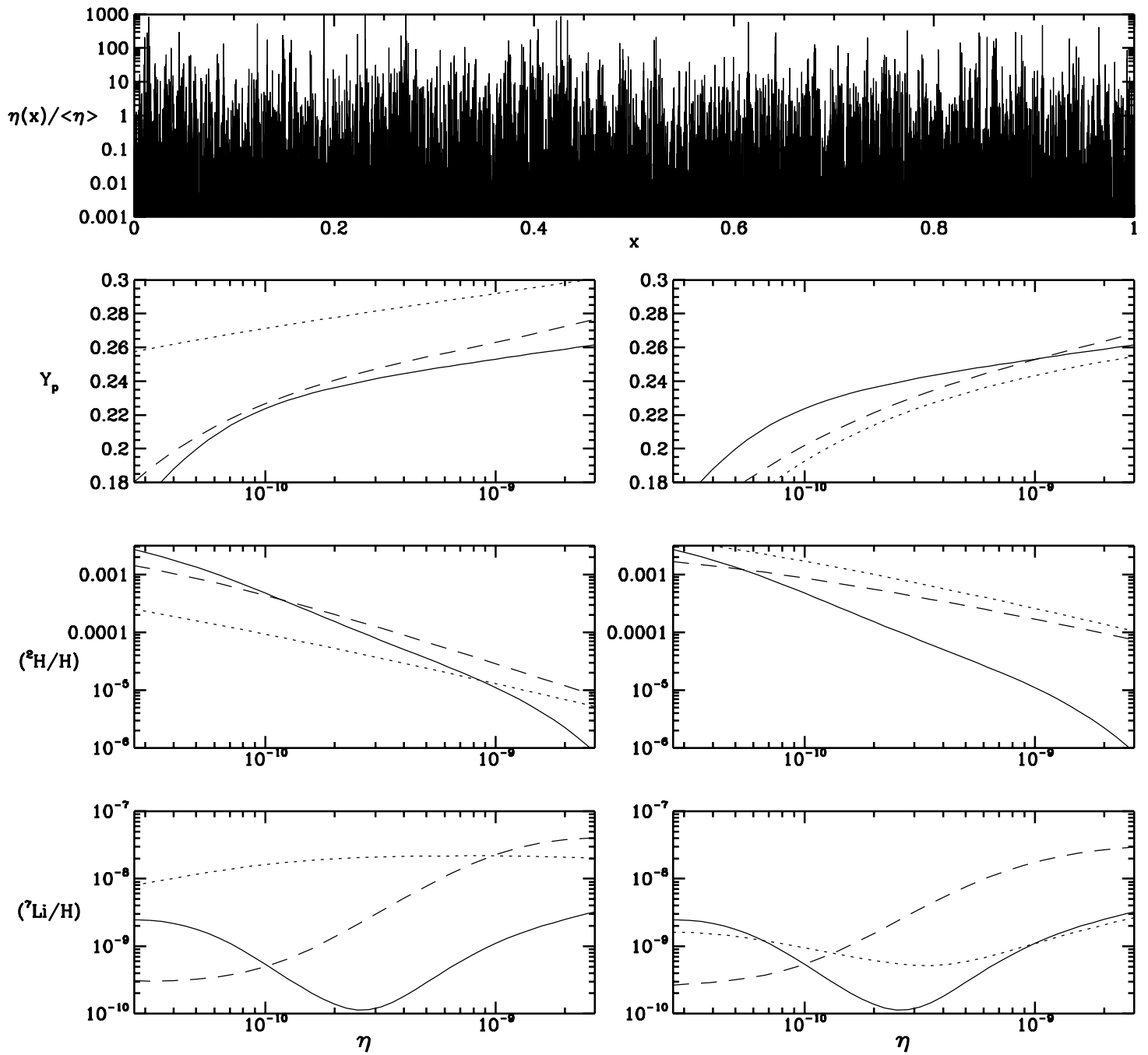


Figure 3

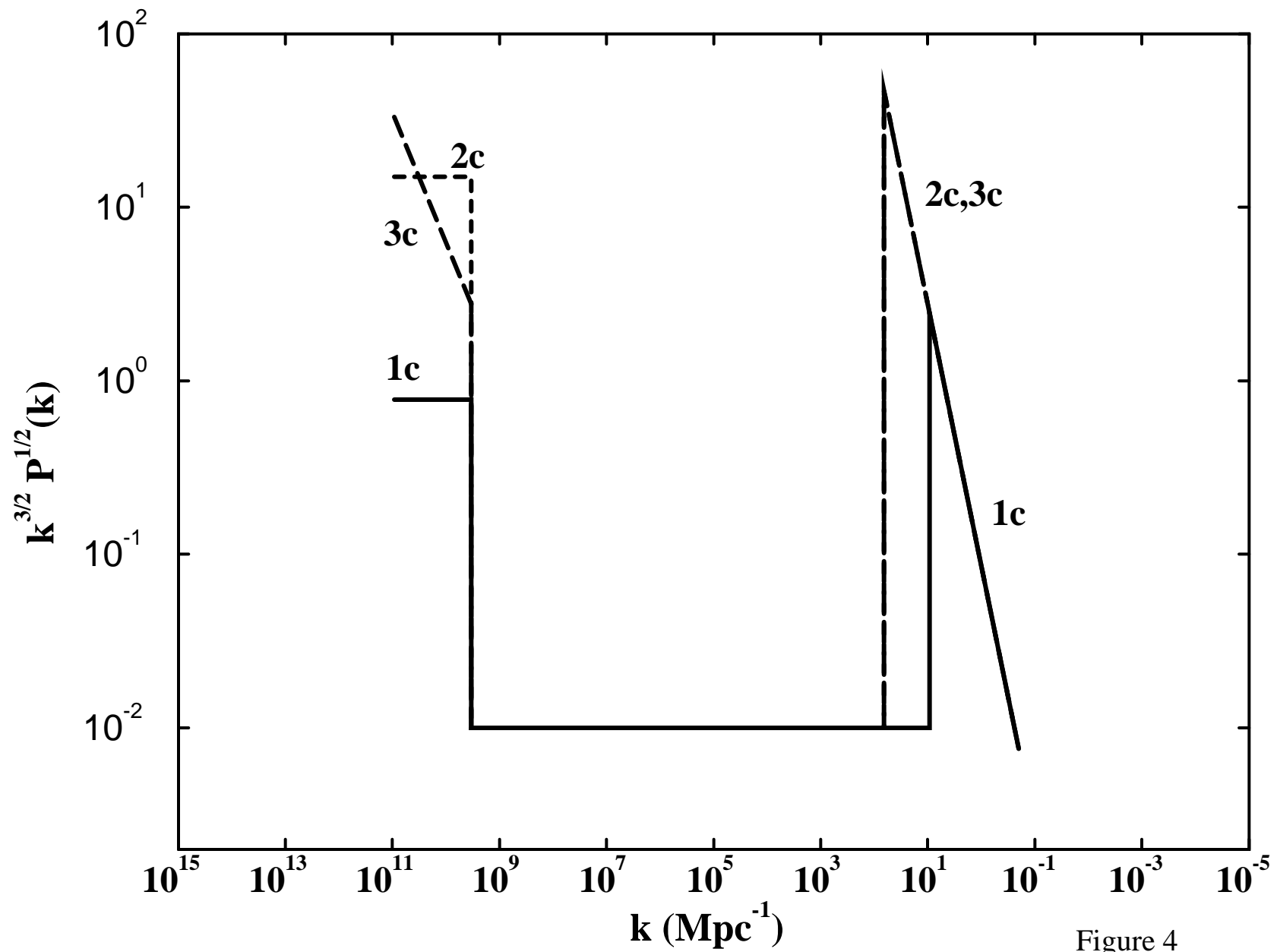


Figure 4